Zinc Deficiency Exacerbates Loss in Blood-Brain Barrier Integrity Induced by Hyperoxia Measured by Dynamic MRI (44477)

MICHAEL D. NOSEWORTHY*,[2] AND TAMMY M. BRAY†,[1]

*Department of Human Biology and Nutritional Sciences, University of Guelph, Guelph, Ontario, Canada N1G 2W1; and †Department of Human Nutrition, The Ohio State University, Columbus, Ohio 43210–1295

Abstract. **Using dynamic Magnetic Resonance Imaging (dMRI), blood-brain barrier (BBB) permeability (k^{PS_p}) and tissue interstitial leakage space (v_e) were evaluated in zinc-deficient (ZnDF) male weanling Wistar rats following 3 days exposure to hyperoxia (85% O_2). Temporal monitoring of T1-weighted MR image changes, following a bolus intravenous injection of gadolinium-DTPA, allowed estimation of BBB integrity. Three-day exposure of hyperoxia caused a marginal loss of BBB integrity, reflected in a slight increase in k^{PS_p} and v_e, observed in both the animals fed adequate zinc (ZnAL) and pair-fed controls (ZnPF). However, zinc deficiency resulted in a significant increase in both k^{PS_p} and v_e, indicating a severely disturbed BBB. In addition MR-visible free water was elevated in ZnDF brains following hyperoxia treatment indicating that a loss of BBB integrity may be associated with neuronal edema. The diminished BBB integrity may be free-radical mediated as the ratio of oxidized to reduced glutathione (GSSG:GSH) was significantly elevated.** [P.S.E.B.M. 2000, Vol 223]

Exposure of the brain to excessive oxidative stress increases the risk of neuronal disorders. Structurally, the brain is well protected. However, the brain is susceptible to oxidative damage due to regionally high concentrations of iron and ascorbate, a high content of polyunsaturated fatty acids, high oxygen consumption, and a relatively low antioxidant capacity (1). An antioxidant nutrient deficiency could further increase the susceptibility of the brain to oxidative stress.

Premature infants are at high risk to excessive oxidative stress. In addition to their developmental immaturity, these newborns frequently have low nutritional status and low antioxidant storage, including zinc (2). To enhance oxygen uptake they are placed into hyperoxic incubators. Elevated environmental oxygen has been shown to be deleterious to the lungs and eyes (3) of premature infants due to excess oxygen radical formation. These infants are also susceptible to a variety of neurological disorders, including cerebral palsy, and other motor and cognitive disorders (4, 5). The brain problems observed might be due, in part, to free radical damage similar to that observed in other tissues.

Disruption of the blood-brain barrier (BBB), a capillary ultrastructural formation that protects the brain (6), could be an initiating event in the etiology of some of the brain disorders observed in the premature infant. We speculate that low zinc status of premature infants could be an important variable exacerbating this brain oxidative damage since zinc acts as an antioxidant important in BBB membrane stability and in the protection of membrane protein thiol groups (7). Zinc is involved in brain phospholipid metabolism (8). Alteration of BBB integrity due to weakened antioxidant defenses and increased oxidative exposure may predispose the brain of premature infants to oxidative damage leading to neurological disorders. In addition, zinc also functions in the brain as a neuromodulator. It may be involved in the regulation of neurotransmission by modulating presynaptic neurotransmitter release.

Financial support for this study was provided by the Natural Sciences and Engineering Research Council of Canada to T.M.B. and by The National Institute of Health to T.M.B. (RO1 NS38315).

[1] To whom requests for reprints should be addressed at 347 Campbell Hall, 1787 Neil Ave, The Ohio State University, Columbus, OH 43210–1295. E-mail: bray.21@osu.edu

[2] Current address for M.D.N.: The Department of Medical Biophysics, University of Toronto, Imaging Research, Sunnybrook & Women's College Health Sciences Center, Room S605, 2075 Bayview Ave., Toronto, Ontario, Canada M4N 3M5. E-mail: mikenose@sten.sunnybrook.utoronto.ca

Received January 27, 1999. [P.S.E.B.M. 2000, Vol 223]
Accepted September 2, 1999.

0037-9727/00/2232-0175$14.00/0

It is difficult to avoid artifacts when one measures the oxidative damage in the brain *ex vivo* since the removed brain is subject to rapid biochemical changes and oxidation. Therefore, we chose to investigate the effects of zinc deficiency and hyperoxia on BBB integrity using dynamic MRI, which permits noninvasive monitoring of changes in the brain over time. To evaluate brain oxidative stress, results were compared to established biochemical indices that may indicate the presence or absence of imbalance in oxidative tone.

Materials and Methods

Animals and Experimental Design. Weanling male, 4-week-old, Wistar rats, 60–70 g (Charles River, St. Constant, Quebec, Canada) were obtained and housed in the University of Guelph Animal Facility according to the Canadian Council on Animal Care. Animals were on a 12-hr light/dark cycle for the entire experiment. Animals were fed and weighed daily.

Animals were given free access to either a zinc-adequate diet (ZnAL; zinc = 100 p.p.m.) or a zinc-deficient diet (ZnDF; zinc < 1 p.p.m.) for 14 days (9). An additional control group, the pair-fed animals (ZnPF), were used to control for the reduced dietary intake exhibited by the ZnDF group. This group received the same amount of food as consumed by the ZnDF group the previous day. The ZnDF group was given deionized, double-distilled water. The other two groups were given tap water. Twelve animals were used for each dietary treatment.

Following the 14-day feeding trial, each group was divided equally into hyperoxia- and normoxia-treated groups. This resulted in $n = 6$ animals for each treatment combination. Animals exposed to normobaric hyperoxia were placed into a Plexiglas chamber fed with a blended mixture of 100% O_2 and compressed air. Gases were blended using a Bird 3800 Microblender (Bird Products Corporation, Palm Springs, CA) to yield chamber effluent flow of 3 liters/min containing 85% O_2 at 1 atmosphere pressure. Oxygen concentration was monitored using a Servomex Oxygen Analyzer OA 570 (Servomex Limited, Crowborough, Sussex, UK). The incubator included containers of boric acid and soda lime to scavenge NH_3 and CO_2, respectively. These were refreshed daily. After 3 days of hyperoxia exposure, BBB integrity was assessed. The animals were sacrificed with Euthansol (0.5 ml of 340 mg/ml sodium pentobarbital). Subsequently blood, *via* cardiac puncture, and whole brains were removed and immediately frozen in liquid nitrogen for analysis of zinc content. In a parallel feeding/hyperoxia trial (same as described above), in which MRI was not performed, levels of brain glutathione (GSH, reduced, and GSSG, oxidized) were determined.

Biochemical Analysis. Using atomic absorption spectrophotometry, brain and plasma zinc were determined according to the method of Hammermueller *et al.* (9). Brains were digested in acid-washed tubes for 48 hr in 0.1*N* nitric acid. Samples were then gently heated to dryness. The resultant was dissolved in 0.1*N* nitric acid and analyzed on a Varian atomic absorption spectrophotometer. Plasma zinc was determined directly from the samples, without sample modification. Zinc content was determined from standard curves of $ZnSO_4$.

Brain samples for enzyme assays were prepared according to Oliver *et al.* (10). All reagents described below were obtained from Sigma Chemical Co. (St. Louis, MO) and stored accordingly prior to use. Whole brains were homogenized (0.1 g brain per ml) in HEPES buffer (10 m*M*, pH = 7.4) containing 137 m*M* NaCl, 0.6 m*M* KCl, 1.1 m*M* K_2HPO_4, 0.6 m*M* $MgSO_4$, and 1.1 m*M* EDTA. To prevent degradation, the protease inhibitors leupeptin (0.5 μg/ml), pepstatin (0.7 μg/ml), aprotinin (0.5 μg/ml), and phenylmethylsulfonyl fluoride (PMSF, 40 μg/ml) were added. Samples were centrifuged at 100,000*g* for 1 hr at 4°C. The supernatant was extracted for use in all assays and protein determination (11).

Total glutathione and GSSG were determined enzymatically using the method of Tietze (12). For total glutathione, an aliquot of homogenized brain tissue was acidified using 5% trichloroacetic acid (TCA). The acidified sample was centrifuged (6000*g*), and an aliquot of the subsequent supernatant was mixed with 0.6 m*M* 5,5′-dithiobis-(2-nitrobenzoic acid) (DTNB, Ellman's Reagent) and GSH reductase (0.32 U, Sigma G-4751, St. Louis, MO). The enzyme reaction was initiated by the addition of 0.2 m*M* NADPH and followed spectrophotometrically at 412 nm. Reaction rates were compared to GSH standards. GSSG was similarly measured, except the sample of brain homogenate was incubated for 20 min in 0.1 *M* KH_2PO_4 buffer (pH = 5.9) containing *N*-ethylmaleimide (NEM). The NEM reacts with GSH to form a stable complex that was removed using affinity chromatography (Sep Pak C18 cartridge #51910, Waters). The remaining GSSG was incubated with GSH reductase and DTNB, and the subsequent product was assayed spectrophotometrically at 412 nm. GSH was calculated from the difference between total and oxidized glutathione. Both GSH and GSSG are expressed in terms of μmol/mg protein in the sample.

Magnetic Resonance Imaging. Animals were anesthetized with isofluorane (2% initially, 1% subsequently; administered using a Fluotec-3 vaporizer). Anesthetic gas delivery was maintained during imaging *via* 7 meters of tubing from the Fluotec-3 vaporizer to the magnet. Imaging was performed using a 2 Tesla SISCO 85/310 animal imaging spectrometer (SISCO, Fremont, CA).

Following MR calibration and brain localization, BBB permeability was assessed using contrast enhanced Dynamic MRI as described by Tofts *et al.* (13, 14). The contrast agent used as a tracer was gadolinium diethylenetriamine pentaacetic acid (Gd-DTPA). This chelate has a molecular weight of 550 Da, osmolality of 1.96 osmol/kg (at 37°C), and a butanol:buffer partition coefficient of 0.0008 (at pH = 7.0) (15). It has been used routinely for the

last decade as a contrast agent in human MRI with zero to minimal side effects. A bolus of Gd-DTPA (0.1 m*M*/kg; Magnevist, Berlex Canada, Montreal) was given *via* an intravenous tail vein catheter, inserted prior to positioning of the animal in the imager. Every 4 min, for 36 min, T1 weighted (TR = 700 ms, TE = 25 ms) coronal images were obtained. Images were acquired using a multislice spin-echo imaging sequence (128 × 256 matrix, 2NEX), with a field of view of 7x 6 cm. The slice thickness was 3.1 mm. As the images did not allow accurate discrimination between brain structures, a region of interest (ROI) was chosen from an area that encompassed the central regions of the brain the size of which was ≈ 5 mm × 5 mm × 3.1 mm thick. This ROI, chosen from a coronal slice through the midbrain, included the periventricular area that has been described as the brain region most sensitive to oxidative stress (5). Each temporal data point was calculated as a mean of all pixels over the ROI. This value was calculated from the same ROI on subsequent images in the time series using an in-house computer program. Capillary permeability to the contrast agent (k^{PSp}) and the volume of the leakage space (v_e) were determined iteratively from the ROI intensity at each time point, using a least squares minimization procedure that employed a Marquardt-Levenberg algorithm. In brief, following a bolus of Gd-DTPA, the spin echo signal at time zero, $S_{SE}(0)$, increases according to the following relationship (13):

$$S_{SE}(t) = S_{SE}(0) \cdot \frac{[\exp(-TE \cdot R_2 \cdot C_t(t))] \cdot \left(1 - \exp\left(\frac{-TR}{T_1^0} + C_t(t) \cdot R_1\right)\right)}{1 - \exp\left(\frac{-TR}{T_1^0}\right)} \quad (1)$$

where $S_{SE}(t)$ is the signal at time = t, following Gd-DTPA injection, TE is the echo time, TR is the repeat time, T_1° is the precontrast T_1 relaxation (1000 ms), R_1 = 4.52 $s^{-1}mM^{-1}$liter, R^2 = 5.66 $s^{-1}mM^{-1}$liter (16), and $C_t(t)$ is the tissue concentration of Gd-DTPA at time t. The Gd-DTPA tissue concentration, $C_t(t)$, is described by:

$$C_t(t) = D \cdot k^{PSp} \cdot \sum_{i=1}^{2} a_i \cdot \frac{\exp(-t \cdot k^{PSp}/v_e) - \exp(-m_i t)}{m_i - (k^{PSp}/v_e)} \quad (2)$$

(17) where D is the tracer dose, a_1 = 3.99 kg/liter, a_2 = 4.78 kg/liter, m_1 = 0.144 min^{-1}, and m_2 = 0.0111 min^{-1} (16). Some assumptions required for this kinetic model are: i) intravenous administration of the IV bolus of Gd-DTPA results in its rapid and homogeneous distribution in plasma, and all tracer within each compartment is well mixed; ii) all Gd-DTPA that leaks into the lesion eventually leaks back to the plasma; iii) tracer diffusion is linearly related to a Gd-DTPA concentration difference across the BBB; iv) the partition coefficient across the BBB is constant; and v) all animals examined have the same plasma curve.

Brain MR-visible water proton density was determined prior to Gd-DTPA enhancement using Volume Selective Spectroscopy (VOSY) (18). Data were acquired from the same ROI as described above, except the region was cubic (4 × 4 × 4 mm^3) rather than rectangular. Other sequence parameters included 16 acquisitions, TR = 5 sec, and TE = 25 ms. The area under the water peak NMR spectral curve was calculated using SISCO software, assuming a Lorentzian lineshape. Peaks were standardized to the VOSY signal peak obtained from a water solution containing $CuSO_4$ (10 m*M*) that was taped to the side of the animal in each scan.

Statistics. There were 12 animals in each of three dietary groups. Following 2 weeks of diet, the animals were subdivided into oxygen treatments (normoxia and hyperoxia) resulting in six treatment combinations with six animals in each experimental treatment group. All statistical analyses were performed using SAS (Cary NC, ver. 6.03). Data were analyzed using the General Linear Models procedure of SAS. The Least Squares Means procedure was implemented to analyze between treatment combinations. The level of significance for all tests was set at $P < 0.05$.

Results

Brain and Plasma Zinc Following Zinc Deficiency and Hyperoxia Exposure. Rats fed a zinc-deficient diet had a markedly reduced weight gain (22.5 ± 2.1 g), relative to zinc-adequate controls (112.1 ± 5.5 g), following the 14-day feeding trial (Fig. 1). This result, concurrent with the result that the ZnDF animals had significantly lower plasma zinc (Fig. 2a) than both ZnAL and ZnPF groups, indicated that the dietary regime was successful at producing rats deficient in zinc. Plasma zinc was no different between ZnAL and ZnPF animals. Physically ZnDF animals exhibited a lack of grooming, resulting in poor condition of the coat and skin. In addition to reduced plasma zinc, a significant decrease was also observed in the brains of the ZnDF animals (Fig. 2b). There was no difference in brain zinc in animals treated with hyperoxia, relative

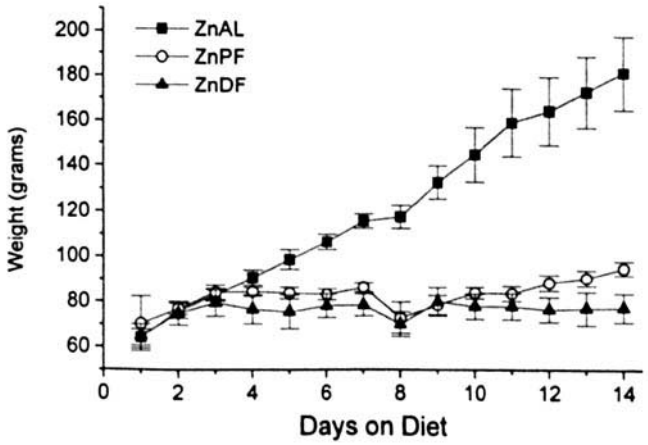

Figure 1. Mean rat weights as a function of time on diet. Each point is a mean (n = 12) ± 1 standard deviation. At the end of 2 weeks the groups were subdivided into hyperoxia- and normoxia-exposed animals resulting in six animals for each treatment combination (ZnAL = *ad libitum* zinc, ZnPF = pair-fed control, ZnDF = zinc deficient).

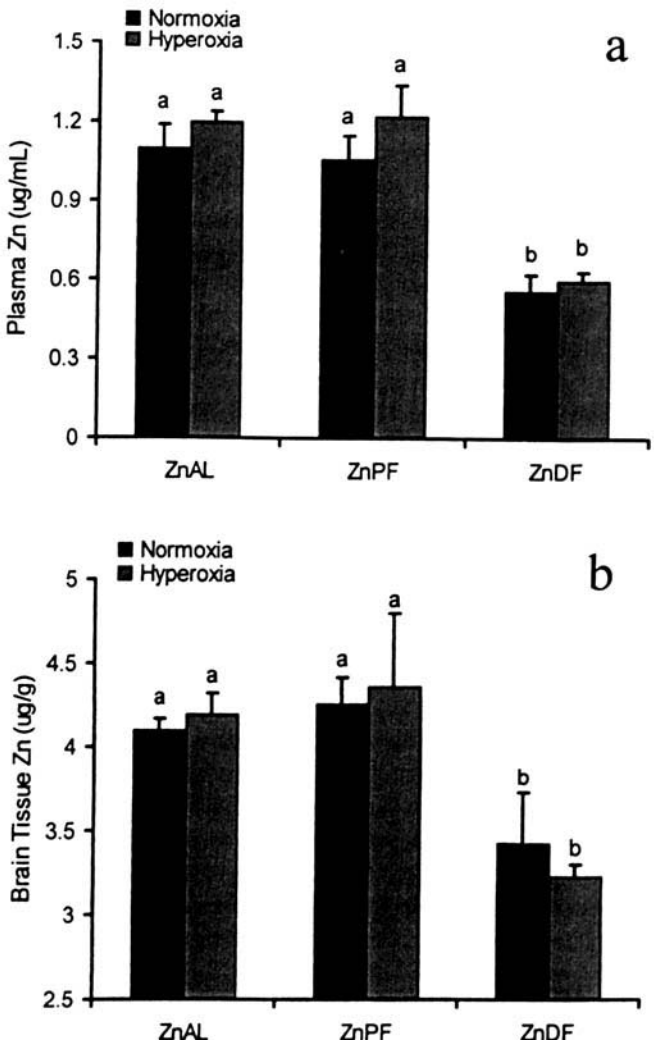

Figure 2. The effect of 2 weeks of zinc deficiency, and subsequent 3 days of hyperoxia, is shown on plasma (a) and brain zinc (b). (ZnAL = *ad libitum* zinc, ZnPF = pair-fed control, ZnDF = zinc deficient). Values are means ± SEM from $n = 6$ rats per treatment combination. Within each graph, bars not containing the same subscript are significantly different ($P < 0.05$) as determined by the Least Squares Means procedure of SAS.

to normoxia controls and hence diet was the only factor that affected brain and plasma zinc.

Magnetic Resonance Imaging of the Blood-Brain Barrier. Gadolinium-enhanced coronal T1-weighted MR images of rats exposed to normoxia (Figs. 3a, 3b, and 3c) and hyperoxia (Figs. 3d, 3e, and 3f) are presented. Images were taken 4 min postgadolinium intravenous injection. Peripheral tissues appeared bright due to the presence of Gd-DTPA, which is permitted ready passage from the blood vessels to the extracellular fluid. While in the blood vascular pool, the influence of Gd-DTPA on surrounding tissue water protons, as detected using T1-weighted spin-echo MR imaging, is minimal. In the brain, enhanced image brightness was indicative of Gd-DTPA interaction with brain extracellular/extravascular water protons, following passage across a leaky BBB. Zinc deficiency, when superimposed with hyperoxia exposure, consistently

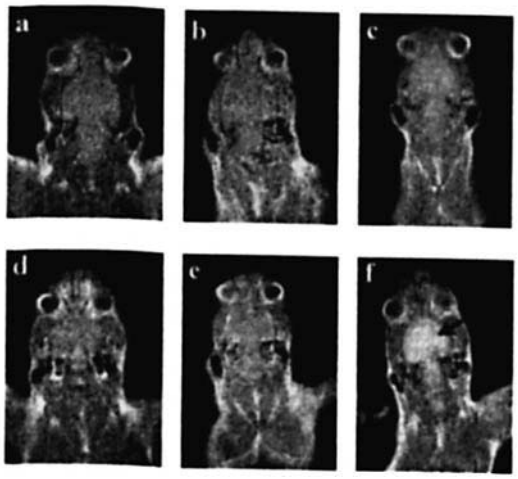

Figure 3. Gd-DTPA enhanced T1-weighted MR images of rat brains. MR images of normoxia-exposed brains of (a) zinc-adequate (ZnAL); (b) pair-fed control (ZnPF); and (c) zinc-deficient (ZnDF) rats; and MR images of brains of (d) ZnAL; (e) ZnPF; and (f) ZnDF rats exposed to 85% oxygen for 3 days. The ZnDF hyperoxia exposed rat brain enhanced most observable as an increased brain signal intensity following Gd-DTPA injection (f).

produced the largest observable enhancement of T1-weighted MR image signal intensity (Fig. 3f). Whole-brain MR T1-weighted signal intensity, at 4 min post-Gd injection, appeared brightest in the ZnDF group after hyperoxia exposure.

Figure 4 depicts the postcontrast enhancement curves, which are the quantitative measurement of whole-brain MR

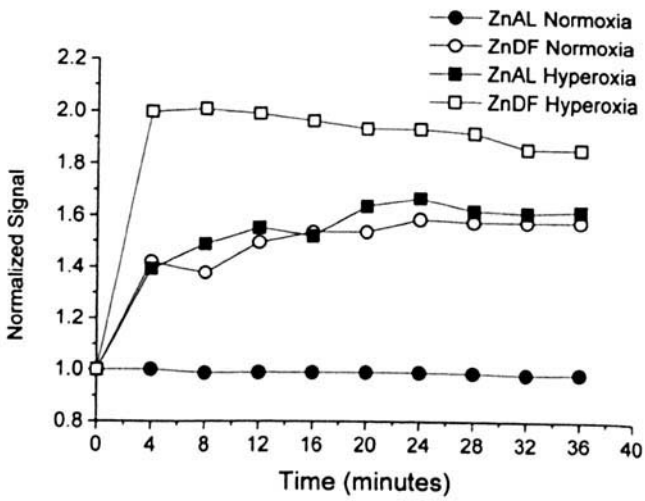

Figure 4. Typical contrast enhancement curves of ZnDF and ZnAL rat brains exposed to 85% and 20% oxygen. Data were obtained from an ROI chosen from an area encompassing the central regions of the brain the size of which was ≈ 5 mm × 5 mm × 3.1 mm thick. Each data point on the plot represents a mean value for all the pixels in the ROI, at each time point. The ZnDF hyperoxia-exposed brain enhanced the fastest and greatest, suggesting the leakiest BBB of all treatment combinations (K^{PS_p} = 0.064/min for this brain). Calculated permeability for the other curves shown was 0.026/min (ZnDF normoxia animal), and 0.029/min (ZnAL hyperoxia-exposed animal). The ZnAL normoxia animal brain did not enhance leading to apparent permeability of ≈ 0 using this method. Pair-fed data are not shown for clarity. In each case MRI signal was normalized to time = 0.

Table I. Effects of Zinc Deficiency on Blood-Brain Barrier Permeability (k^{PSp}) and Capillary Leakage Space (v_e) in Rats Exposed to Hyperoxia

Oxidative stress	ZnAL		ZnPF		ZnDF	
	v_e (%)	k^{PSp} (min^{-1})	v_e (%)	k^{PSp} (min^{-1})	v_e (%)	k^{PSp} (min^{-1})
20% O_2	≈ 0.0	≈ 0.0	0.2 ± 0.1	0.005 ± 0.003	3.9 ± 0.9	0.017 ± 0.010
85% O_2	12.4 ± 2.3	0.028 ± 0.007	10.7 ± 3.3	0.027 ± 0.013	19.6 ± 2.9	0.043 ± 0.030

Note. Values are means ± SEM for n = 6 rats per treatment combination (ZnAL = *ad libitum* control, ZnPF = pair-fed control, ZnDF = zinc-deficient).

T1-weighted signal intensity at 4 min post-Gd injection. The ZnDF brains had the most rapid enhancement, indicative of a leakier BBB. Because increases in brain intensity are time-dependent, kinetic analysis allows calculation of the permeability (k^{PSp}) of the BBB and barrier leakage space (v_e), presented in Table I. The brains of control rats (ZnAL and normoxia) were not leaky and did not cause an apparent change in signal intensity ($k^{PSp} \approx 0.0$, $v_e \approx 0.0$). In these animals, the model did not converge to fit the data because the brain signal did not increase. Although there is some minimally finite degree of permeability in the assumed healthy BBB of these animals, the method is not sensitive enough to detect such a slight value. Fitted parameters in these animals were assigned the value of approximately zero (i.e., ≈ 0.0). Hyperoxia exposure caused an increase in BBB permeability (k^{PSp} = 0.028/min). The v_e, or the percentage volume of the extracellular space, into which contrast agent has leaked, was 12.4%. Similar observations were found in the ZnPF group where the normoxia animals had essentially a nonleaky BBB, and hyperoxia resulted in k^{PSp} = 0.027/min and v_e = 10.7%. There was a slight loss in BBB integrity in the brain of the ZnDF group. Superimposing oxidative stress (hyperoxia) dramatically increased the permeability of the BBB. The rate of Gd-DTPA transfer, through the leaky BBB, into the brain extracellular space was 0.043/min, and 19.6% of the brain interstitial space was involved.

Relative Brain Water Content. Relative brain MR-visible water content in hyperoxia-exposed animals, normalized to the normoxia controls, is shown in Figure 5. The ZnDF rats exposed to 3 days of hyperoxia had the highest brain water content of all treatment groups examined. There was no significant difference between ZnAL and ZnPF brains.

Brain content of GSH was dependent upon both zinc and hyperoxia exposure (Fig. 6a). GSSG, however, was dependent upon all main effects parameters, diet, hyperoxia, and their interaction. Examination of specific treatment combinations showed that only the ZnAL animals exhibited a significant rise in brain GSH following hyperoxia. In diet-restricted animals (ZnPF) hyperoxia resulted in a slight, but highly significant, elevation of GSSG ($P < 0.0015$). The ZnDF animals showed a further significant increase in GSSG. The highest GSSG content was found in ZnDF hyperoxia-treated brains. This value was significantly higher ($P < 0.0001$) than all other treatment combinations. The ratio of GSSG to GSH was significantly elevated in ZnDF animals, relative to controls (Fig. 6b). This was increased further following hyperoxia treatment.

Discussion

Magnetic resonance methods have been used for the examination of various organs and tissues, including brain. These techniques have proven invaluable in the diagnosis of brain disorders such as tumors and cerebrovascular disease. However, there has been minimal use of these techniques in the study of nutritional sciences where the use of these methods has focused primarily on body composition (19, 20), brain assessment of phenylketonuria (21, 22), and the neurotoxicity of manganese following chronic total parenteral nutrition (23). The use of MR techniques in the examination of the effects of a nutrient deficiency, and its interaction with oxidative stress, is limited. In our lab we

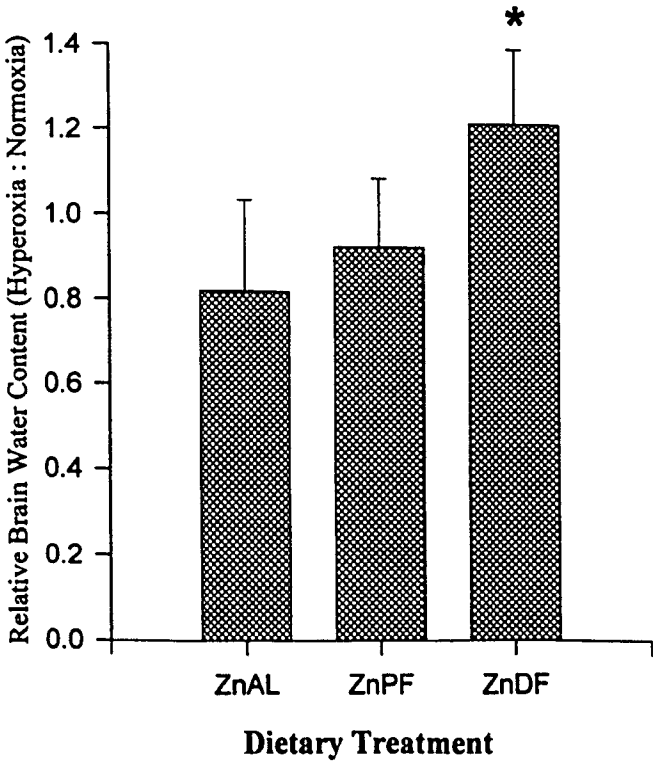

Figure 5. Brain water content of zinc-deficient hyperoxia (85% O_2)-treated rats expressed in terms of normoxia exposure. (ZnAL = *ad libitum* Zn; ZnDF = zinc deficient; ZnPF = pair-fed control). Values are means ± pooled SEM from n = 6 rats per treatment combination. (* = significantly different from the other two groups, $P < 0.05$).

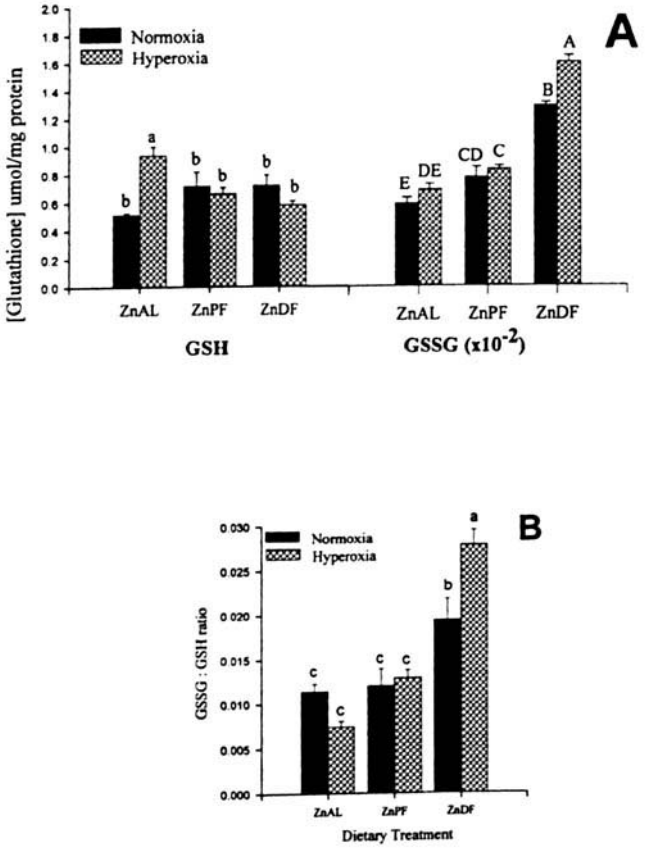

Figure 6. Levels of reduced (GSH) and oxidized glutathione (GSSG) in brains of weanling rats exposed to hyperoxia are shown in (a). The combination of both diet and hyperoxia was significant in altering GSH ($P < 0.0007$). Hyperoxia alone was a significant factor determining GSSG ($P < 0.0004$). Glutathione content is expressed per mg total protein. (b) The ratio of oxidized to reduced glutathione. Both diet ($P < 0.0001$) and the association of diet with hyperoxia exposure ($P < 0.0037$) were deemed significant. Values are expressed as a mean ± SEM ($n = 6$). (ZnAL = zinc *ad libitum* diet; ZnPF = pair-fed control; ZnDF = zinc-deficient diet; similar letters above error bars indicate lack of significance).

have previously demonstrated MR-detectable lung damage in zinc deficiency (24) and copper deficiency (25). Now we report that MR techniques clearly demonstrate that zinc deficiency exacerbates the loss of BBB integrity induced by hyperoxia. This is suggested to be free-radical mediated since an elevated GSSG:GSH ratio was concurrently observed.

Premature infants, exposed to prolonged periods of hyperoxia, are sensitive to a myriad of problems including bronchopulmonary dysplasia (BPD) and retrolental fibroplasia, two disorders attributed to oxygen free radicals (3). In addition ≈ 5%–15% develop cerebral palsy, and an additional 25%–50% exhibit less prominent neurological deficit (5). Behavioral and intellectual skills are also developmentally delayed in these children. For example depressed cognitive development and behavioral problems have been observed (26), and in one study, a 48% increase in the requirement for special educational interventions has been noted (27). Brain damage may be the result of oxidative damage caused by free radicals during hyperoxia exposure combined with an increased susceptibility due to the developmental immaturity of their free radical defenses. Damage to the brain may initially occur at the BBB, the protective boundary between the brain and plasma. This structure is particularly vulnerable to oxidative damage (6). Under prolonged conditions of hyperoxia exposure (1 week at 85% O_2) we have previously demonstrated, using Gd-DTPA–enhanced MRI, that the BBB becomes weakened (28). We report here that BBB integrity was weakened under conditions that are similar to those experienced by the premature infant, namely zinc deficiency and hyperoxia exposure (Table I). Although the zinc deficiency produced in this study was extreme relative to the zinc status of premature infants, it does not rule out the possibility that BBB disruption may be involved in the pathogenic process in some of the more extremely delicate premature infant brains.

The susceptibility of the BBB to oxidative damage may be due to the high influx of oxygen, relatively low antioxidant capacity, and the high membrane PUFA content (29). Also, the endothelial cells comprising the BBB have specialization making them more susceptible to oxidative damage (6): [e.g., i) endothelial cell NO• and $O_2•^-$ production; ii) high levels of endothelial cell xanthine oxidase, which also produces $O_2•^-$; and iii) easily disrupted transferrin receptors (transport iron into the brain) that release the prooxidant iron that spontaneously catalyzes the formation of •OH radicals through the Fenton reaction]. Oxidation of this membrane is known to alter fluidity, enzyme activity, and transmembrane ion fluxes (29) suggesting a free radical imbalance may influence the integrity of the BBB, causing increased permeability. This is supported by data from rat experiments showing that dietary enhancement with antioxidants protects against ischemia-mediated BBB disruption (30). In another study, enhancement of antioxidant capacity by increasing CuZn superoxide dismutase (CuZnSOD) and chelating excess iron with desferoxamine, inhibited BBB alterations caused by pneumococcal meningitis (31).

One antioxidant function of zinc is its role as a membrane stabilizer. In addition to prevention of the disrupting effects of lipid peroxidation and membrane protein oxidation, zinc acts to stabilize membranes through various mechanisms. It has been shown that zinc promotes membrane skeletal and cytoskeletal protein associations, blockage of membrane channels caused by toxins and amphipathic molecules, and antagonism of the adverse effects of Ca^{2+} (32). Also, zinc acts to protect protein thiol groups from oxidation, and it competes with prooxidants, iron and copper, diminishing their oxidation potential. Zinc is also a component of CuZnSOD that converts potentially destructive $O_2•^-$ to H_2O_2 (7). Therefore zinc should afford BBB membrane protection from oxidative stress. In non-BBB capillaries permeability appears increased in zinc deficiency (8). Our study appears to corroborate this finding that the zinc-deficient animals had a weakened BBB. The added stress of hyperoxia exacerbated the permeability in the ZnDF animals. Biochemically the elevation in GSSG:GSH

observed in the ZnDF hyperoxia-exposed animals is suggestive of increased brain oxidative stress that has been demonstrated in other tissues under similar circumstances (24).

Changes in BBB integrity potentially result in edema and alterations in brain metabolism and energy status (32). It has been demonstrated that alterations in BBB integrity can alter brain water content due to osmolarity differences between blood plasma and the brain extracellular space (33). For example, brain tumors and infections can cause changes in BBB integrity and result in local regions of brain edema in humans, as shown by MRI. In the present study, brain water content was significantly increased in the ZnDF animals following hyperoxia treatment (Fig. 4), the treatment group having the weakest BBB.

In our study zinc deficiency resulted in significantly reduced brain zinc. Only in some studies has this been similarly reported following zinc deficiency (34, 35). In one study, concurrently with a decrease in brain zinc, a 24% increase in brain calcium was also observed (36). Elevation of cellular calcium is known to cause cell death. ZnDF may result in neuronal damage through impairment of nonantioxidant functions. For example the lack of zinc in stabilizing glutaminergic synaptic vesicles could possibly result in release of excess glutamate, a known neurotoxin when in excess (37). Also, zinc deficiency has been shown to produce alterations in behavior (38) and memory (39). There has been suggestion that an apparent decrease in brain zinc may be due to poor tissue preparation for elemental analysis. It may be better to perfuse the brain with zinc-free saline to remove residual blood. Since brain blood volume is between 2% and 4% of wet weight the omission of this step likely was not the cause of the 20% reduction in brain zinc observed here.

A correlation between some clinical neurological disorders and zinc status has been observed. For example, zinc levels have been elevated in brains of Parkinson's patients and epileptics, and decreased in Alzheimer's disease, depression, and schizophrenia (40). Although it appears that zinc is important as a prophylactic against neuronal damage, there has been recent suggestion that pharmacological doses of zinc exacerbates the pathogenesis of Alzheimer's disease (41). *In vitro* studies demonstrated that zinc precipitated β-amyloid proteins. The relationship of the integrity of BBB in Alzheimer's disease and zinc homeostasis in the brain has not been examined. One of the possible mechanisms may be that the BBB in Alzheimer's disease has been weakened and that a pharmacological dose of zinc passes unregulated into the brain accelerating β-amyloid precipitation.

It appears that zinc deficiency superimposed with oxidative stress predisposes the brain to damage mediated through BBB disruption. Because zinc is an antioxidant and the condition of hyperoxia results in elevated levels of tissue $O_2^{\bullet -}$, and because the BBB has been shown previously to be sensitive to oxidative stress (6), it is suggested that loss of BBB integrity is free-radical mediated. This is supported by our finding of a significant elevation in the ratio of GSSG:GSH. Free-radical mediated disruption of this protective layer results in an increase in brain extracellular water. These results suggest that neurological damage observed in individuals who have an extremely low zinc status during prolonged hyperoxia exposure, may be due in part to antioxidant, possibly zinc deficiency and oxidative stress imposed by high oxygen exposure. This finding may be relevant to the most extremely delicate premature infants.

1. Carney JM, Starke-Reed PE, Oliver CN, Landum RW, Cheng MS, Wu JF, Floyd RA. Reversal of age-related increase in brain protein oxidation, decrease in enzyme activity, and loss of temporal and spatial memory by chronic administration of the spin trapping compound N-tert-butyl-α-phenylnitrone. Proc Natl Acad Sci U S A **88**:3633–3636, 1991.
2. Tyrala EE. Zinc and copper balances in preterm infants. Pediatrics **77**:513–517, 1986.
3. Kelly FJ. Free radical disorders of preterm infants. Br Med Bull **49**:668–678, 1993.
4. Graziani LJ, Mitchell DG, Kornhauser M, Pidcock FS, Merton DA, Stanley C, McKee L. Neurodevelopment of preterm infants: Neonatal neurosonographic and serum bilirubin studies. Pediatrics **89**:229–234, 1992.
5. Volpe JJ. Brain injury in the premature infant: Is it preventable? Pediatr Res **27**:S28–S33, 1990.
6. Betz L. Oxygen free radicals and the brain microvasculature. In: Partridge WM, Ed. The Blood–Brain Barrier. New York: Raven Press, p303, 1993.
7. Bray TM, Bettger WJ. The physiological role of zinc as an antioxidant. Free Radic Biol Med **8**:281–291, 1990.
8. Cunnane SC. Zinc Clinical and Biochemical Significance. Boca Raton, FL: CRC Press, p99, 1988.
9. Hammermueller JD, Bray TM, Bettger WJ. Effect of zinc and copper deficiency in microsomal NADPH-dependent active oxygen generation in rat lung and liver. J Nutr **117**:894–901, 1987.
10. Oliver CN, Starke-Reed PE, Stadtman ER, Liu GJ, Carney JM, Floyd RA. Oxidative damage to brain proteins, loss of glutamine synthetase activity, and production of free radicals during ischemia/reperfusion-induced injury to gerbil brain. Proc Natl Acad Sci U S A **87**:5144–5147, 1990.
11. Lowry OH, Rosebrough NJ, Farr AL, Randall RJ. Protein measurement with the Folin phenol reagent. J Biol Chem **193**:265–275, 1951.
12. Tietze F. Enzymatic method for quantitative determination of nanogram amounts of total and oxidized glutathione: Applications to mammalian blood and other tissues. Anal Biochem **27**:502–522, 1969.
13. Tofts PS, Kermode AG. Measurement of the blood-brain barrier permeability and leakage space using dynamic MR imaging. 1. Fundamental concepts. Magn Reson Med **17**:357–367, 1991.
14. Tofts PS, Berkowitz B, Schnall MD. Quantitative analysis of dynamic Gd-DTPA enhancement in breast tumours using a permeability model. Magn Reson Med **33**:564–568, 1995.
15. Weinmann HJ, Gries G, Speck U. Gd-DTPA and low osmolar Gd chelates. In: Runge VM, Ed. Enhanced Magnetic Resonance Imaging. Toronto: CV Mosby Co., p74, 1989.
16. Weinmann JH, Brasch RC, Press WR, Wesbey GE. Characteristics of gadolinium DTPA: A potential NMR contrast agent. Am J Roentgenol **142**:619–624, 1984.
17. Tofts PS. Modeling tracer kinetics in dynamic Gd-DTPA MR imaging. J Magn Reson Imag **7**:91–101, 1997.
18. Kimmich R, Hoepfel D. Volume selective multipulse spin-echo spectroscopy. J Magn Reson **72**:379–384, 1986.
19. Cefalu WT, Wang ZQ, Werbel S, Bell Farrow A, Crouse JR III,

Hinson WH, Terry JG, Anderson R. Contribution of visceral fat mass to the insulin resistance of aging. Metab Clin Exp **44**:954–959, 1995.
20. Fuller MF, Fowler PA, McNeill G, Foster MA. Imaging techniques for the assessment of body composition. J Nutr **124**:1546S–1550S, 1994.
21. Jones SJ, Turano G, Kriss A, Shawkat F, Kendall B, Thompson AJ. Visual evoked potentials in phenylketonuria: Association with brain MRI, dietary state, and IQ. J Neurol Neurosurg Psychiatry **59**:260–265, 1995.
22. Moller HE, Vermathen P, Ullrich K, Weglage J, Koch HG, Peters PE. *In vivo* NMR spectroscopy in patients with phenylketonuria: Changes of cerebral phenylalanine levels under dietary treatment. Neuropediatrics **26**:199–202, 1995.
23. Fredstrom S, Rogosheske J, Gupta P, Burns LJ. Extrapyramidal symptoms in a BMT recipient with hyperintense basal ganglia and elevated manganese. Bone Marrow Transplant **15**:989–992, 1995.
24. Taylor CG, Towner RA, Janzen EG, Bray TM. MRI detection of hyperoxia-induced lung edema in zinc-deficient rats. Free Radic Biol Med **9**:229–233, 1990.
25. Taylor CG, Bray TM. Increased lung copper-zinc-superoxide dismutase activity and absence of magnetic resonance imaging–detectable lung damage in copper-deficient rats exposed to hyperoxia. J Nutr **121**:467–473, 1991.
26. Weisglas-Kuperus N, Koot HM, Baerts W, Fetter WP, Sauer PJ. Behaviour problems of very low-birthweight children. Dev Med Child Neurol **35**:406–416, 1993.
27. Ross G, Lipper EG, Auld PA. Educational status and school-related abilities of very low-birthweight, premature children. Pediatrics **88**:1125–1134, 1991.
28. Noseworthy MD, Bray TA. Effect of oxidative stress on brain damage detected by MRI and *in vivo* ^{31}P-NMR. Free Radic Biol Med **24**:942–951, 1998.
29. Shukla A, Shukla R, Dikshit M, Srimal RC. Alterations in free radical scavenging mechanisms following blood-brain barrier disruption. Free Radic Biol Med **15**:97–100, 1993.
30. Tasdemiroglu E, Christenberry PD, Ardell JL, Chronister RB, Taylor AE. Effects of antioxidants on the blood-brain barrier and postischemic hyperemia. Acta Neurochir **131**:302–309, 1994.
31. Pfister HW, Koedel U, Lorenzl S, Tomasz A. Antioxidants attenuate microvascular changes in the early phase of experimental pneumococcal meningitis in rats. Stroke **23**:1798–1804, 1992.
32. Bettger WJ, O'Dell BL. Physiological roles of zinc in the plasma membrane of mammalian cells. J Nutr Biochem **4**:194–207, 1993.
33. Rapoport SI. A model for brain edema. In: Inaba Y, Klatzo I, Spatz M, Eds. Brain Edema. Proceedings of the Sixth International Symposium. Berlin: Springer-Verlag, p59, 1985.
34. Roth HP, Kirchgessner M. Calmodulin, zinc, and calcium concentration in tissues of zinc- and calcium-deficient rats. J Trace Elem Electrolytes Health Dis **2**:73–78, 1988.
35. Oteiza PI, Hurley LS, Lonnerdal B, Keen CL. Effects of marginal zinc deficiency on microtubule polymerization in the developing rat brain. J Nutr **118**:735–738, 1988.
36. Dubinsky JM. Examination of the role of calcium in neuronal death. Ann N Y Acad Sci **679**:34–42, 1993.
37. Oka A, Belliveau MJ, Rosenberg PA, Volpe JJ. Vulnerability of oligodendroglia to glutamate: Pharmacology, mechanisms, and prevention. J Neurosci **13**:1441–1453, 1993.
38. Golub MS, Takeuchi PT, Keen CL, Gershwin ME, Hendrickx AG, Lonnerdal B. Modulation of behavioral performance of prepubertal monkeys by moderate dietary zinc deprivation. Am J Clin Nutr **60**:238–243, 1994.
39. Guidolin D, Polato P, Venturin G, Zanotti A, Mocchegiani E, Fabris N, Nunzi MG. Correlation between zinc level in hippocampal mossy fibers and spatial memory in aged rats. Ann N Y Acad Sci **673**:187–193, 1992.
40. Dreosti IE. Neurobiology of zinc. In: Mills CF, Ed. Zinc and Human Biology. New York: Springer-Verlag, p235, 1989.
41. Bush AI, Pettingell WH, Multhaup G, Paradis MD, Vonsattel JP, Gusella JF, Beyreuther K, Masters CL, Tanzi RE. Rapid induction of Aß amyloid formation by zinc. Science **265**:1464–1467, 1994.